Desalination and Water Treatment
www.deswater.com

doi: 10.1080/19443994.2014.995136

53 (2015) 3711–3723
March

Taylor & Francis
Taylor & Francis Group

Removal of methyl orange from aqueous solution via adsorption on cork as a natural and low-coast adsorbent: equilibrium, kinetic and thermodynamic study of removal process

Fouad Krika*, Omar el Farouk Benlahbib

Department of Process Engineering, University of Laghouat, BP 37G, Laghouat 03000, Algeria, Tel. +213 7 77 26 57 50; email: f.krika@lagh-univ.dz (F. Krika)

Received 17 May 2014; Accepted 27 November 2014

ABSTRACT

In this study, the cork powder was used as adsorbent to remove methyl orange (MO) from aqueous solutions by adsorption. Batch experiments were conducted to study the effect of reaction parameters on the adsorption of the dye such as: contact time, initial concentrations of solution, adsorbent dosage, solution pH, and temperature; consequently, optimum condition of adsorption was obtained. The surface properties and structure of cork were measured by some techniques including: Scanning electron microscope, Fourier transform infrared spectrometry, point of zero charge, and Boehm titration method. Adsorption capacity of cork for MO is 16.66 mg g^{-1} at 298 K under the optimum condition of pH of 2, cork dosage of 5.00 g l^{-1}, particle size of d<0.08 mm, and contact time of 240 min. The kinetic data obtained from different experiments were analyzed using three kinetic models namely pseudo-first-order, pseudo-second-order, and Elovich kinetics models. Among the kinetics models studied, the pseudo-second-order model was the best applicable model to describe the adsorption of MO onto cork. Freundlich and Langmuir models were used to analyze the obtained experimental data. In comparison, Langmuir model was understood to be a better fit for the experimental data than Freundlich model. The value of Gibbs free energy of adsorption (ΔG°) was found to be −14.96 kJ mol^{-1}; the negative value indicated the spontaneity of the adsorption process of MO onto cork. The values of (ΔH°) and (ΔS°) were found to be −11.71 kJ mol^{-1} and −10.93 J mol^{-1} K^{-1}, respectively. The thermodynamics parameters indicated that the adsorption of MO onto cork was spontaneous and exothermal.

Keywords: Cork; Adsorption; Methyl orange; Kinetics; Thermodynamics

1. Introduction

Water pollution is a common problem worldwide. It has become more and more serious, especially regarding dye ions. Dye ions, mainly from dyeing industries, have become a serious threat to human beings and the aquatic ecosystem, due to their toxicity [1]. Methyl orange (MO) is a representative contaminant in industrial wastewater and shows poor biodegradability [2], hence, several methods such as membrane [3], electrochemical [4], coagulation/flocculation [5], biological [6–8], and adsorption [9–13] have been used to treat wastewater containing this pollutant. The adsorption process has been shown to be an

*Corresponding author.

effective technique with its efficiency, capacity, and applicability on a large scale to remove dyes as well as having the potential for regeneration, recovery, and recycling of adsorbents [14–19]. And activated carbon is the most effective adsorbent with high surface and can be regenerated, but it is limited due to the high operation costs, and this is a major economic consideration in any large-scale remediation application [20] that has led to a search for cheaper substitutes. Natural biomasses that are available in large quantities may have potential as inexpensive adsorbents. Due to their low cost, they can be discarded without expensive regeneration. Adsorbents such as coal [21], fly ash [22], wood [23], agricultural wastes (bagasse pith, maize cob, coconut shell, rice husk, etc.), and cotton wastes have been tried as an absorbent for color removal [22,24–27].

A literature review showed that cork has not been used before to remove acid dyes from colored wastewater. In this study, cork was used as an adsorbent to remove MO from aqueous solution. Effective parameters such as adsorbent dosage, dye concentration, inorganic anion (salt), pH, and temperature were investigated on dye removal. Kinetic, isotherm, and thermodynamic studies were conducted to evaluate the adsorption capacity of cork.

2. Experimentals

2.1. Chemicals and materials

The cork powder used was supplied by the Algerian company "EPE/ JIJEL Etancheite's SPA." The cork powder was washed several times with double-distilled water and dried at 110°C for 3 h. Particle size fractions were obtained by sieving, and the experiments were carried out with the size fractions with particle diameters of (d_1: <0.08; d_2: 0.08–0.1; d_3: 0.1–0.16, and d_4 :0.16–0.2 mm). These different fractions were used for the adsorption studies.

Analytical grade chemicals are used in this experiment. MO (Fig. 1) was supplied by Merck.

A stock solution of MO (1,000 mg l^{-1}) was prepared. Experimental solutions of desired concentration were obtained by successive dilutions with double-distilled water. The pH of the solutions was adjusted using reagent-grade dilute sulfuric acid (0.1 N) and sodium hydroxide (0.1 N).

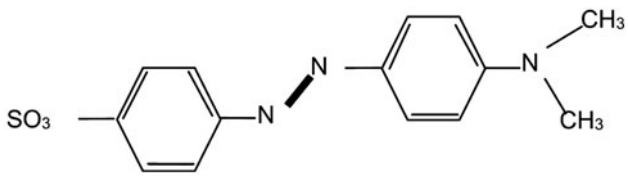

Fig. 1. Structure of methyl orange (MO).

2.2. Analysis method

The concentrations of the dye in the sample solution were measured in a Shimadzu spectrophotometer (6101) UV–vis. All measurements were performed at the maximum absorbency visible wave length (465 nm). In alkaline media, dye exists as an equilibrium mixture of undissociated and dissociated dye forms; to simplify analyses, measurements were recorded at the isosbestic point as the extinction coefficients for the two forms were identical.

2.3. Surface studies

The functional groups of the cork were detected by FTIR spectroscopy (Shimadzu 8400 s). The point zero charge (pH_{PZC}) was used to determine the point where the density of electrical charge is zero. The solid addition method [28] was used to determine the point zero charge of the adsorbent. SEM Analysis was performed using an environmental scanning electron microscopy (Quanta 200). Boehm titration method [29] was used to determine the amount of acidic or basic functional groups on the surface of the adsorbent.

2.4. Adsorption studies

The adsorption studies were carried out by batch process. The dye adsorption was performed in a set of Erlenmeyer flasks where a solution of MO with certain concentration of amount and, then, cork were introduced. When it reached equilibrium, the solution was centrifuged, the absorbance of supernatants was determined by spectrophotometer, and then, the concentration was calculated by the standard curve equation.

The amount of MO adsorbed at equilibrium per unit mass of adsorbent was determined according to the following equation:

$$q_e = \frac{(C_0 - C_{e)} \cdot V}{m} \quad (1)$$

where m is the mass of adsorbent (g), V is the volume of the solution (l), C_0 is the initial concentration of MO (mg l^{-1}), C_e is the equilibrium concentration of the adsorbate (mg l^{-1}) in solution, and q_e is the MO quantity adsorbed at equilibrium (mg g^{-1}).

2.5. Adsorption isotherm

Adsorption isotherm data were described by the two most widely used models. The Langmuir model is expressed by the following equation [30]:

$$q_e = \frac{q_m b C_e}{1 + b C_e} \quad (2)$$

and the Freundlich model is expressed by the following equation [31]:

$$q_e = K_F \, C_e^{\frac{1}{n}} \quad (3)$$

where C_e is the equilibrium concentration in the liquid phase (mg l^{-1}) and q_e the equilibrium sorption capacity of sorbent (mg g^{-1}). Parameter q_m represents the maximum sorption capacity (mg g^{-1}) with monolayer coverage on the sorbent particle, while, b, the Langmuir constant related to the free energy of sorption (l mg^{-1}). K_F is the sorption capacity constant and n the Freundlich constant for surface heterogeneity.

2.6. Thermodynamic studies

The thermodynamic parameters such as change in Gibbs free energy (ΔG°), enthalpy (ΔH°), and entropy (ΔS°) were determined using the following equations [32]:

$$\Delta G = -RT \; Ln \; K_C \quad (4)$$

$$K_C = \frac{C_A}{C_S} \quad (5)$$

$$\text{Ln } K_C = \frac{\Delta S^\circ}{R} - \frac{\Delta H^\circ}{RT} \quad (6)$$

$$\Delta G^\circ = \Delta H^\circ - T\Delta S^\circ \quad (7)$$

where R (8.314 J/mol K), T (K), C_A, C_S, and K_c (l g^{-1}) are the gas constant, the absolute temperature, the amount of dye adsorbed on the adsorbent of the solution at equilibrium (mg l^{-1}), the equilibrium concentration of the dye in the solution (mg l^{-1}), and the standard thermodynamic equilibrium constant, respectively.

3. Results and discussion

3.1. Surface studies

The FTIR spectroscopy of cork before and after MO adsorption is shown in Fig. 2(a) and (b), respectively. It was seen that the peaks (Fig. 2(a)) could be assigned as follows: 3,432 cm^{-1} (γ OH), (2,922 and 2,851) cm^{-1} (γ C–H) asymmetric and symmetric in C–H, CH_2, (γ C=O), 1,735 cm^{-1} and 1,631 cm^{-1}, (δ C–O) 1,036 cm^{-1}, where γ represented a stretching vibration and δ, a blending vibration. An obvious change was observed on the spectrum of cork-adsorbed MO. The adsorption bands at 3,432, 2,922, 2,851, 1,735, 1,631, and 1,036 cm^{-1} (Fig. 2(a)) had shifted, respectively, to 3,412, 2,912, 2,842, 1,730, 1,620, and 1,025 cm^{-1} due to MO adsorption (Fig. 2(b)). These shifts might be attributed to ion exchange associated with carboxylate and hydyroxylate anions, suggesting that acidic groups, carboxyl and hydroxyl, were predominant contributors in dye ions uptake.

The result in Fig. 3 shows that the surface charge of cork at pH 4.6 was zero. Hence, the pH_{pzc} of cork was 4.6. The pH_{pzc} of adsorbent indicated that the surface of adsorbent is positively charged since the pH of solution (pH 2) is less than pH_{pzc}.

Boehm titration method was used to determine the surface chemistry and the amount of functional groups such as phenolic, lactonic, and carboxylic groups of the cork. The experimental results of the titration method are presented in Table 1. Obviously, the total amount of acidic groups (2.113 mmol g^{-1}) is much higher than that of the basic groups (0.946 mmol g^{-1}), indicating the cork surface is acidic, which resulted from the presence of major acidic groups.

Scanning electron microscopic photographs of cork showed (data not shown) that it has microscopic features different from other lignocellulosic materials. Its structure is formed by hollow polyhedral prismatic cells, which have a honeycomb shape when observed from the radial direction (relative to the tree trunk) and rectangular when viewed from transversal directions, resembling a brick wall.

3.2. Effect of initial pH

The pH of dye solution plays an important role in the whole adsorption process and, particularly, in the adsorption capacity, influencing the surface charge of the adsorbent, the degree of ionization of the dye present in the solution, and the dissociation of functional groups on the active sites of the adsorbent, but also the solution dye chemistry [33–35].

The adsorption behavior of MO on cork was studied using various initial pHs varying from 2 to 10. The variation of equilibrium MO uptake with initial pH is given in Fig. 4 at about 100 mg l^{-1} initial dye concentration at 298 K. As seen from the figure, the adsorption capacity of MO was slightly decreasing

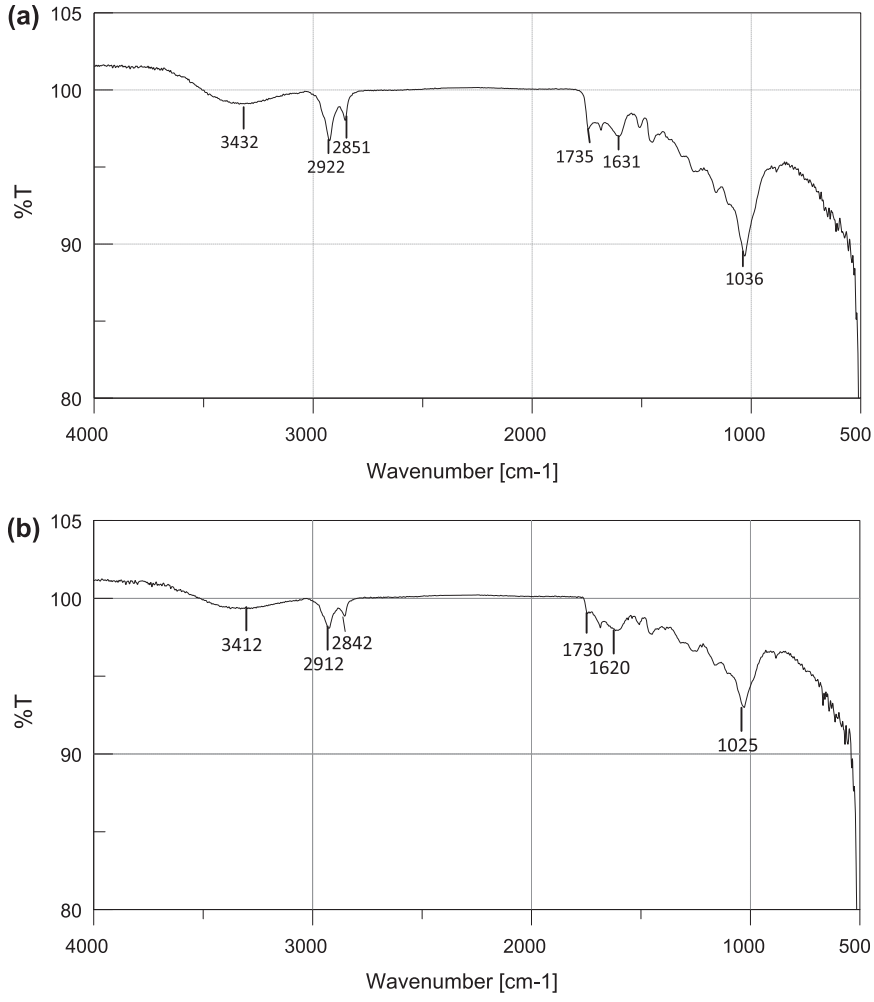

Fig. 2. FTIR spectrum of: (a) cork and (b) MO-cork loaded.

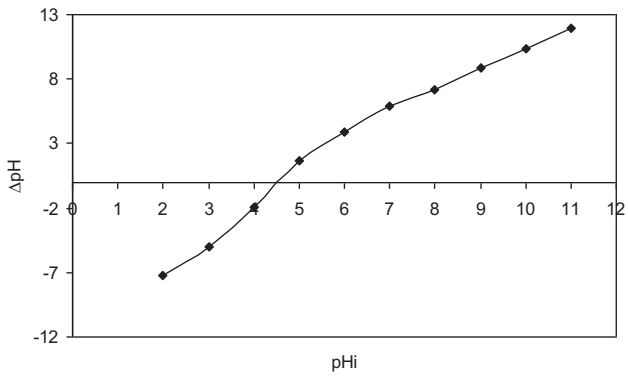

Fig. 3. Determination of pH_{pzc} of the cork.

within the pH range 2–4, then, suddenly decreased as the pH of the solution increased to 10. Maximum adsorption of dye occurs at acidic pH (pH 2). Cork

Table 1
Boehm results of cork

Active sites	mmol g^{-1}
Total acidic sites	2.113
Carboxylic	0.962
Lactone	0.637
Phenolic	0.514
Total basic sites	0.946

comprises various functional groups, such as hydroxyl and carbonyl groups [36], which are affected by the pH of solutions. This means that the predominant charges on the cork at acidic pH are positive and, because of having SO_3^- group in the structure of dye, it seems that the dominant mechanism of the adsorption is electrostatic attraction. At pH 2, a considerable high electrostatic attraction exists between the positively charged surface of the adsorbent and dye

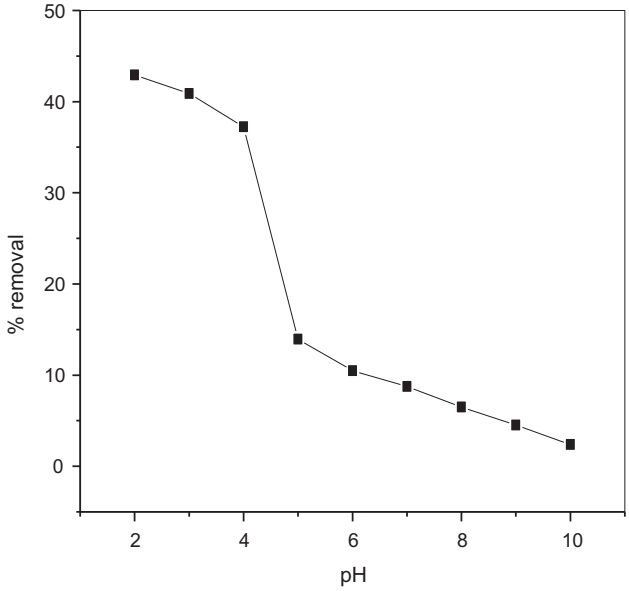

Fig. 4. Effect of pH on the adsorption of MO onto cork (C_0 = 100 mg l^{-1}, m = 1 g, d < 0.08 mm, T = 25°C, and contact time = 240 min).

anions, due to the ionization of functional groups of adsorbent and negatively charged anionic dye molecules. As the pH of the system increases, the number of negatively charged sites increases. A negatively charged site on the adsorbent does not favor the adsorption of anionic dyes due to the electrostatic repulsion [37,38]. Moreover, lower adsorption of MO at alkaline pH is due to the presence of excess OH^- ions destabilizing anionic dye and competing with the dye anions for the adsorption sites [39]. Since the adsorbent show high adsorption at pH 2, all further studies were carried out at this pH.

3.3. Effect of particles size

The contact surface between any adsorbent and the liquid phase plays an important role in the phenomena of adsorption [36]. Four different particle sizes viz. $d_1 < 0.08$, $0.08 < d_2 < 0.1$, $0.1 < d_3 < 0.16$, and $0.16 < d_4 < 0.2$ mm were selected for batch adsorption experiments. The influence of the adsorbent particle size was investigated at constant pH 2, 100 mg l^{-1} of MO at 298 K. According to Fig. 5, it is found that the percentage removal of MO increases with the reduction in the diameter of the particles. The decrease in the dye removal with increase in the particle size is a result of decreased surface area of the adsorbent. The maximum percentage elimination of MO (i.e. 41.91%) was reached using the fine particles (d_1<0.08 mm).

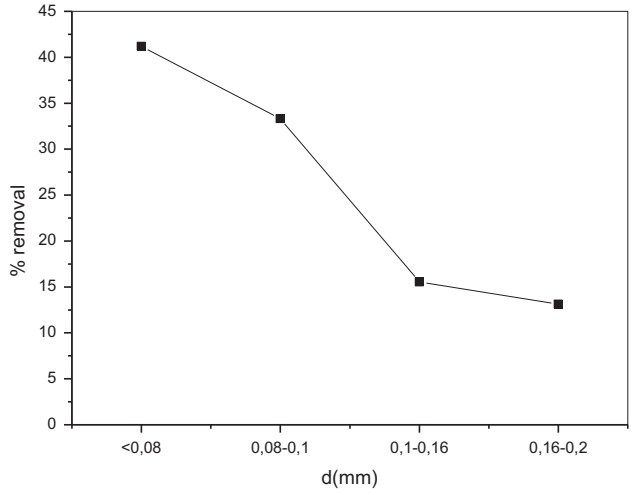

Fig. 5. Effect of particle size (C_0 = 100 mg/l, m = 1 g, pH = 2, T = 25°C, and contact time = 240 min).

3.4. Effect of adsorbent dosage

In order to evaluate the effect of cork dose on MO removal, various amounts of cork ranging from 1.0 to 5 g l^{-1} were taken, and adsorption of MO was achieved at 298 K. The initial concentration of the dye in solution was 100 mg l^{-1}, pH 2. Fig. 6 shows the percentage of MO removal by cork. The results demonstrate that the removal percentage is positively correlated with the amount of cork added. A rapid removal rate increases with the addition of cork when the dosage is less than 2 g l^{-1} and then the percentage removal increases slowly. When the amount of

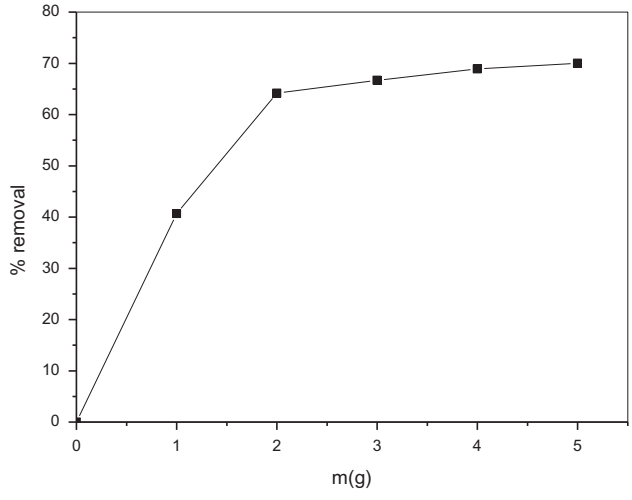

Fig. 6. Effect of adsorbent dosage on MO removal by cork (C_0 = 100 mg l^{-1}, d < 0.08 mm, pH = 2, T = 25°C, and contact time = 240 min).

adsorbent added is 5 g l^{-1}, the highest removal is almost reached (71.04%). An increase in adsorption may be concluded due to the increase in the adsorbent surface and, therefore, more active functional groups result in the availability of more adsorption sites [40]. Consequently, 5 g l^{-1} was used as optimal amount for further experiments.

3.5. Effect of initial concentration, contact time, and temperature on MO adsorption

The effect of initial concentration and contact on MO adsorption was examined at three concentration levels (20, 50, and 100 mg l^{-1}). Fig. 7 shows results performed at ambient temperature using 5 g l^{-1} of adsorbent, pH 2, and with a contact time of 240 min. As can be seen from Fig. 7, the amount of the dye adsorbed onto cork increased from 2.45 to 9.35 mg g^{-1} with increase in the initial dye concentration from 20 to 100 mg l^{-1}. It is because a higher initial concentration provides an important driving force to overcome all resistances of the dye between the aqueous and solid phases, thus increasing the uptake. In addition, increasing the initial dye concentration increases the number of collisions between dye ions and the surface area of cork, which enhances the adsorption process [41].

The influence of temperature (298, 308, and 318 K) on the equilibrium adsorption capacity of absorbent is displayed in Fig. 8. The adsorption of MO was achieved at an adsorbent dose of 5 g l^{-1} initial dye concentration of 50 mg l^{-1} and pH 2.0.

It can be observed that the adsorption capacity was reduced with the increasing temperature, indicating that the adsorption process of MO onto cork is exothermic in nature.

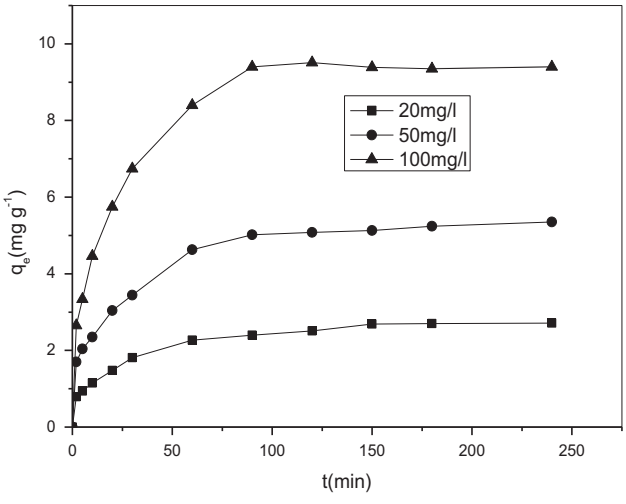

Fig. 7. Effect of initial dye concentration on dye removal by cork (contact time = 240 min, pH 2, d < 0.08 mm, m = 5 g l^{-1}, and T = 298 K).

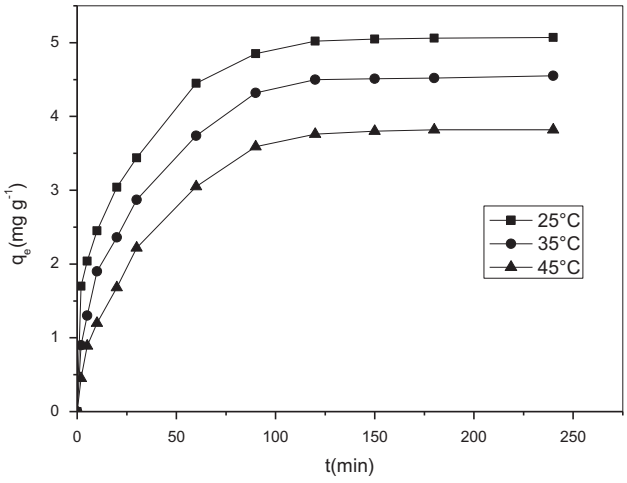

Fig. 8. Effect of temperature on dye removal by cork (C_0 = 50 mg l^{-1}, m = 5 g l^{-1}, contact time = 240 min, pH 2, and d < 0.08 mml).

The decrease in adsorbed amounts with an increase in temperature is probably due to the weakening of adsorptive forces between the active sites on cork and MO species, and also between adjacent MO molecules on the adsorbed phase [42].

The adsorption capacities of cork were 5.02, 4.50, and 3.76 mg g^{-1} at 298, 308, and 318 K, respectively. The optimum temperature for MO adsorption on cork was found to be 298 K within the temperature range studied.

Equilibrium time is one of the most important parameters in the design of economical wastewater treatment systems [43]. The results show (Fig. 7) that with increasing MO concentration, the time required to reach equilibrium increased accordingly. For initial dye concentrations of 20, 50, and 100 mg l^{-1}, the times reaching equilibrium were 30, 90, and 120 min, respectively. At low initial concentrations, the MO adsorption by cork was very intense and reached equilibrium very quickly. However, during the adsorption process, the adsorbent surface was progressively blocked by dye molecules, becoming covered after some time. The hindrance enhanced with increasing dye concentration, and thus the time for adsorption equilibrium increased accordingly.

3.6. Effect of electrolyte (NaCl) concentration

It was important to discuss the effect of salt ionic strength in the adsorption of MO onto cork because dyeing wastewater usually contains high salt

concentration. The effect of NaCl with different concentrations ranging from 10 to 50 g l^{-1} on the dye removal efficiencies of cork is demonstrated in Fig. 9. A seen in Fig. 9, the presence of inorganic salt has significantly influenced the adsorption capacity of cork. It can be observed that adsorption of MO decreased with increasing NaCl concentration. The presence of electrolyte may cause the neutralization of surface charge of adsorbent while competing with MO for surface adsorption. With the increasing ionic strength, the adsorption capacity decreases due to screening of the surface charges.

3.7. Adsorption isotherms

A model isotherm graph for the adsorption of MO at 298, 308, and 318 K is shown in Fig. 10 and the corresponding model parameters along with correlation coefficients are given in Table 2.

Comparisons between the correlation coefficients of two isotherm models that equilibrium data were well represented by the Langmuir isotherm model were observed.

The values of q_m and b calculated from Langmuir plots were found to be 16.66 mg g^{-1} and 0.026 l mg^{-1} for the experiments carried out at 298 K. The values of both q_m and b decreased with a rise in the solution temperature. The values of q_m decreased from 16.66 to 9.40 mg g^{-1}, when the solution temperature increased from 298 to 318 K. The decreasing trend was observed for the values of b depending upon the temperature of solution. The decrease in the values of q_m and b with temperature indicates that the MO are favorably adsorbed by cork at lower temperatures, which shows that the MO adsorption phenomenon is exothermic.

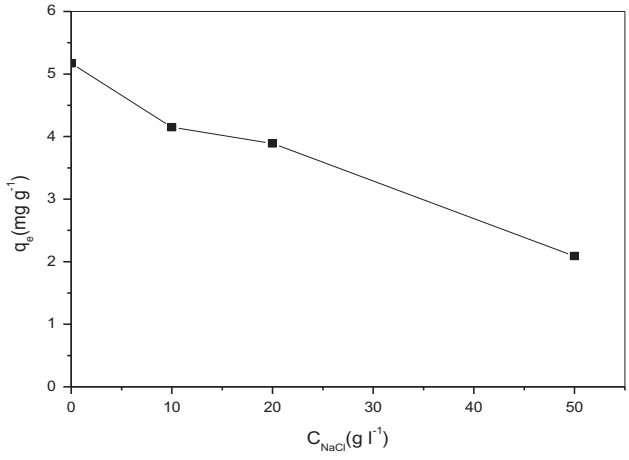

Fig. 9. Effect of salt (NaCl) concentration for MO adsorption on cork (C_0 = 50 mg l^{-1}, m = 5 g l^{-1}, contact time = 120 min, pH 2, and d < 0.08 mm).

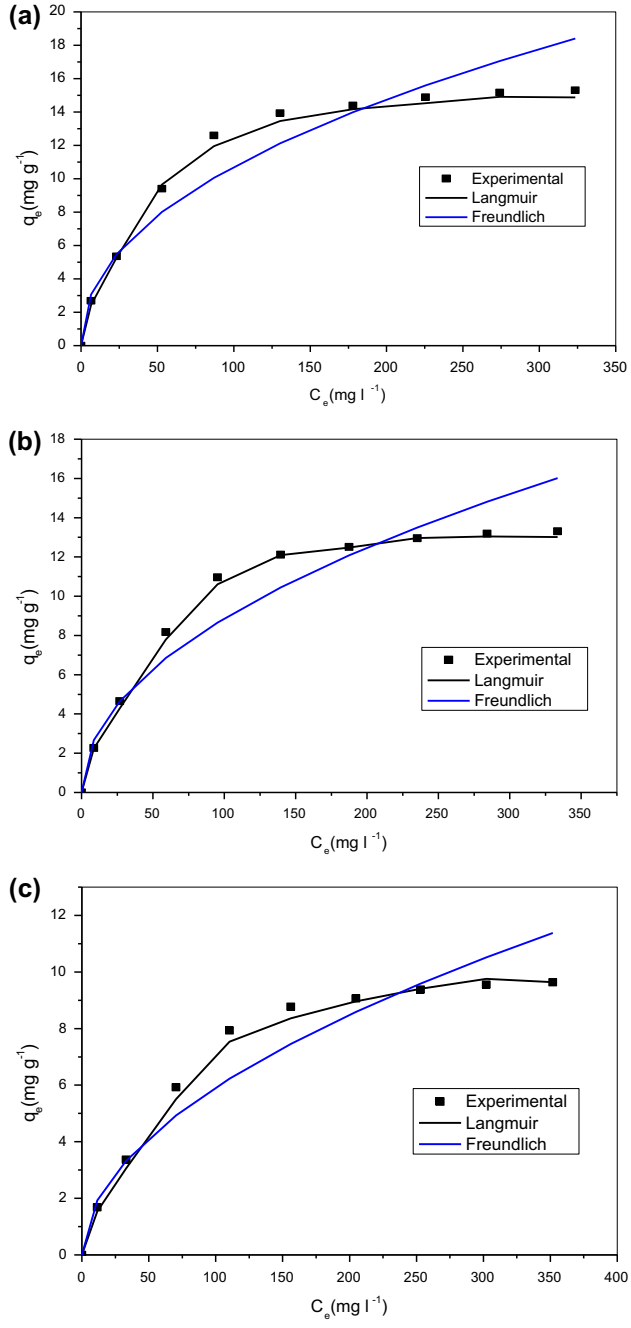

Fig. 10. Adsorption isotherms and the nonlinear fitted curves of two isotherm models (a) 25°C, (b) 35°C, and (c) 45°C at pH 2.

The maximum adsorption capacity is compared in Table 3 with the data reported by other authors for MO Adsorption. As can be seen, the maximum MO adsorption value of cork is higher than those reported in the literature. This comparison indicates the great

Table 2
Langmuir and Freundlich constants for adsorption of MO by cork

Temperature (K)	Langmuir			Freundlich		
	q_m (mg g^{-1})	b (l mg^{-1})	R	K_F	n	R
298	16.66	0.026	0.996	1.29	2.17	0.880
308	15.62	0.011	0.995	0.93	2.03	0.861
318	9.40	0.008	0.993	0.54	1.91	0.839

Table 3
Maximum adsorption capacities of cadmium from aqueous media using various adsorbents

Adsorbents	q_m (mg g^{-1})	References
Algerian cork	16.66	This study
Bottom ash	3.6	[44]
Activated alumina	9.8	[45]
Skin almonds	20.2	[46]
Activated clay	15.85	[47]
Chitosan	9.9	[48]
De-oiled soya	3.62	[49]
Modified wheat straw	50.4	[50]
Carbon nanotubes	51.8	[51]

potential of cork for the removal of MO from wastewater.

In order to find out the feasibility of the isotherm, the essential characteristics of the Langmuir isotherm can be expressed in terms of dimensionless constant separation factor R_L by the Eq. (4) [52]:

$$R_L \frac{1}{1 + bC_0} \tag{8}$$

$R_L > 1$ Unfavorable adsorption
$0 < R_L < 1$ Favorable adsorption
$R_L = 0$ Irreversible adsorption
$R_L = 1$ Linear adsorption

where b is the Langmuir constant (l mg^{-1}) and C_0 is the initial MO concentration (mg l^{-1}). The R_L values between 0.087 and 0.65 indicate that the process is favorable adsorption. These results demonstrate that it is monolayer adsorption on the structurally homogeneous cork, where all the adsorption sites are identical and energetically equivalent and where, the adsorption occurs at specific homogeneous sites within the adsorbent

3.8. Adsorption kinetics

Kinetic studies the mechanism of adsorption that is important for the efficiency of the process.

In order to evaluate the kinetic mechanism for the adsorption of MO on cork biomass at different temperatures (298, 308, and 318 K) and initial dye concentrations (298, 308, and 318 K), pseudo-first-order [53], pseudo-second-order [54], and Elovich [55] models were employed. A good correlation of the kinetic data explains the adsorption mechanism of the dye ions on the solid phase.

Pseudo-first-order model is generally expressed as follows:

$$\log(q_e - q_t) = \log q_e - \frac{k_1}{2.303} t \tag{9}$$

where q_e is the amount of dye ions adsorbed per unit weight of adsorbent at equilibrium, i.e. adsorption capacity (mg g^{-1}), q_t is the amount of adsorbate adsorbed (mg g^{-1}) at any time t, and k_1 is the rate constant. By plotting $\log(q_e - q_t)$ vs. t at different temperatures (298, 308, and 318) (Fig. 11) and different initial concentrations of the solution (Fig. 12), the values of q_e and k_1 were calculated from the slope and intercept,

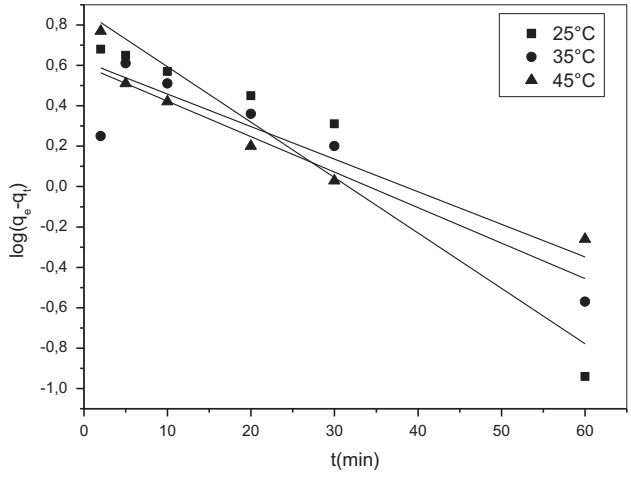

Fig. 11. Pseudo-first-order kinetics for MO adsorption at different temperatures ($C_0 = 50$ mg l^{-1}, $m = 5$ g l^{-1}, $d < 0.08$ mm, and pH 2).

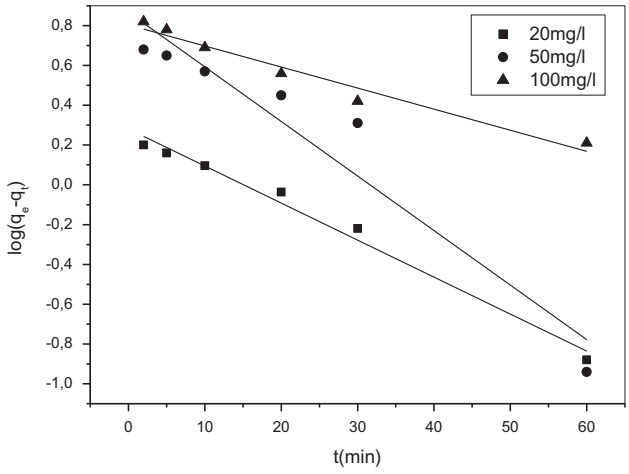

Fig. 12. Pseudo-first-order kinetics for MO adsorption at different concentrations ($T = 25$°C, $m = 5$ g l^{-1}, $d < 0.08$ mm, and pH 2).

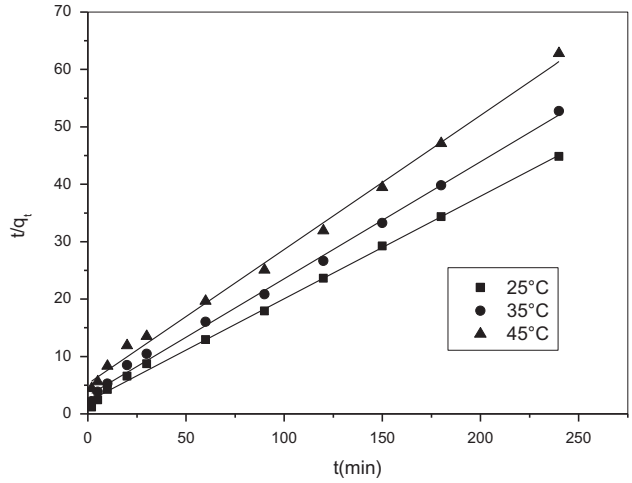

Fig. 13. Pseudo-second-order kinetics for MO adsorption at different temperatures ($C_0 = 50$ mg l^{-1}, $m = 5$ g l^{-1}, $d < 0.08$ mm, and pH 2).

and the correlation coefficient(R) was calculated and is shown in Table 4. The values of the correlation coefficient R for the pseudo-first-order model changed in the range of 0.93 to 0.98. Furthermore, the experimental values of $q_{e,exp}$ (mg g^{-1}) are far from the calculated $q_{e,cal}$ (mg g^{-1}). This suggests that the adsorption of MO onto cork did not follow the pseudo-first-order kinetic model, and it is not a diffusion-controlled phenomenon.

Pseudo-second-order rate model is given as follows:

$$\frac{t}{q_t} = \frac{1}{k_2\ q_e{}^2} + \frac{1}{q_e} t \tag{10}$$

where k_2 is the rate constant. The q_e and k_2 values can be obtained from the slopes and intercepts of plots of t/q_t vs. t which are illustrated in Figs. 13 and 14 (Table 5). The correlation coefficients (R) of linear plots at different concentrations and temperatures are higher than 0.999, which suggest that the adsorption of MO onto cork follows the pseudo-second-order kinetic model.

The simple Elovich model has been also successfully used to describe second-order kinetic assuming that the actual solid surfaces are energetically heterogeneous, and the linear form of this equation is given by:

$$q_t = a + b \ln\ t \tag{11}$$

Table 4
Kinetic parameters for pseudo-first-order kinetic model

Pseudo-first-order kinetic model				$q_{e,exp}$(mg g^{-1})
T(K)	k_1	q_e(mg g^{-1})	R^2	
298	0.063	7.36	0.927	5.02
308	0.04	3.96	0.820	4.51
318	0.037	4.16	0,904	3.82
C_0(mg l^{-1})				
20	0.042	1.90	0.986	2.68
50	0.063	7.36	0.927	5.02
100	0.024	6.30	0.965	9.39

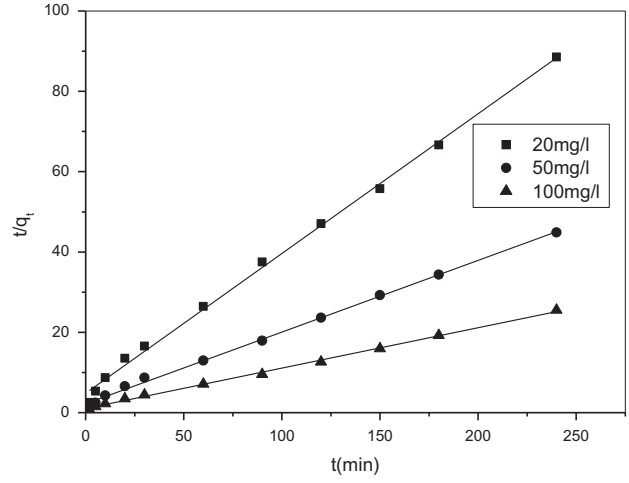

Fig. 14. Pseudo-second-order kinetics for MO adsorption at different concentrations ($T = 25$°C, $m = 5$ g l^{-1}, $d < 0.08$ mm, and pH 2).

Table 5
Kinetic parameters for pseudo-second-order kinetic model

Pseudo-second-order kinetic model				
T(K)	k_2	q_e(mg g^{-1})	R^2	$q_{e,exp}$(mg g^{-1})
298	0.014	5.59	0.998	5.02
308	0.013	4.90	0.997	4.51
318	0.011	4.04	0.995	3.82
C_0(mg l^{-1})				
20	0.025	2.87	0.997	2.68
50	0.014	5.59	0.998	5.02
100	0.010	9.92	0.998	9.39

By plotting q_t vs. ln t at different temperatures (298, 308, and 318) (Fig. 15) and different initial concentrations (20, 50 and 100 mg l^{-1}) (Fig. 16) the initial adsorption rate a and the desorption constant b were calculated from the intercept and the slope of the straight line. The kinetic constants are collected in Table 6. The values of R^2 indicate that the correlation of Elovich kinetics equation was more moderate than that of pseudo-first-order model, but poorer than that of pseudo-second-order model.

Based on the R^2 values and a comparison between the experimental and calculated qe values, it can be seen that the kinetic of MO adsorption onto cork followed a pseudo-second-order model with correlation coefficient higher than 0.99. Besides, the equilibrium adsorption capacity increased as the initial dye concentration increased. It was also found that the variations of the adsorption rate seemed to have a decreasing trend with increasing initial dye concentration. Moreover, the adsorption rate decreased with

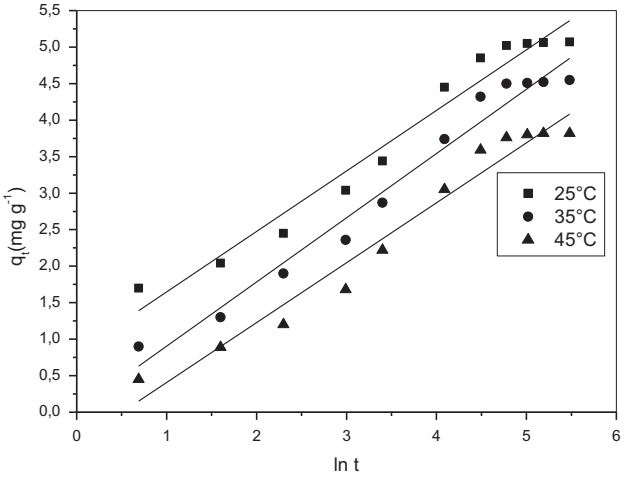

Fig. 15. Elovich kinetics for MO at different temperatures (C_0 = 50 mg l^{-1}, m = 5 g l^{-1}, d < 0.08 mm, and pH 2).

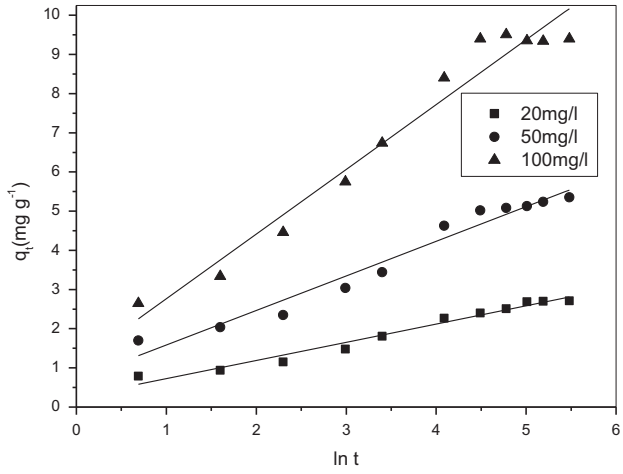

Fig. 16. Elovich kinetics for MO at different concentrations (T = 25°C, m = 5 g l^{-1}, d < 0.08 mm, and pH 2).

Table 6
Kinetics parameters for Elovich kinetics model

Elovich kinetic model				
T(K)	a	b	R^2	$q_{e,exp}$(mg g^{-1})
298	0.817	0.829	0.966	5.02
308	0.022	0.880	0.973	4.51
318	−0.415	0.820	0.967	3.82
C_0(mg l^{-1})				
20	0.259	0.464	0.973	2.68
50	0.70	0.882	0.962	5.02
100	1.107	1.653	0.963	9.39

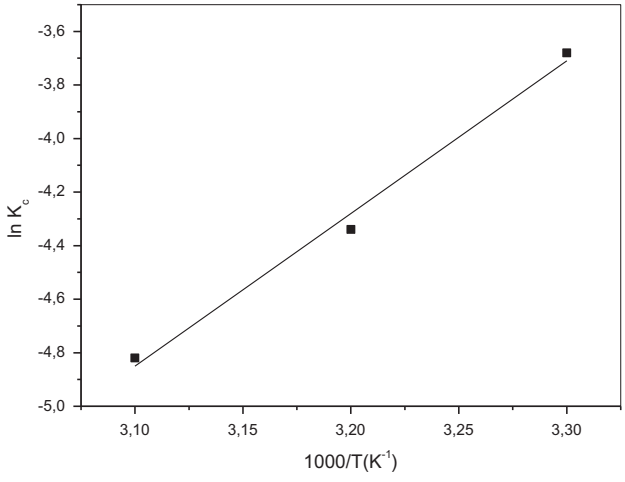

Fig. 17. Plot of ln K_c vs. 1/T for MO adsorption on cork.

Table 7
Thermodynamic parameters of the MO adsorption onto cork at different temperatures

T(K)	ΔG° (kJ mol^{-1})	ΔS° (J mol^{-1} K^{-1})	ΔH° (kJ mol^{-1})	R
298	−14.96	−10.93	−11.71	0.998
308	−15.07			
318	−15.18			

increase in solution temperature. It is probably due to change of mechanism of MO adsorption onto cork upon changing the temperature.

3.9. Thermodynamics of the adsorption process

A plot of ln K_C vs. 1/T gives a straight line (Fig. 17) and the values of ΔH°, ΔS°, and ΔG° are summarized in Table 7. The negative values of ΔH° for MO removal confirm that the dye adsorption process was exothermic in nature. Negative value of change in standard entropy (ΔS°) reflects the decreased randomness at the solid–solution interface during the adsorption of dye on cork. The negative values of ΔG° indicate the feasibility of the process and the spontaneous nature of the adsorption. The change in free energy for physisorption is between −20 and 0 kJ/mol, but chemisorption is in a range of −80 to −400 kJ/mol [56]. The values of ΔG^0 obtained in this study are within the ranges of −20 and 0 kJ/mol, indicating that the physisorption is the dominating mechanism.

4. Conclusion

In this study, cork was considered as low-coast adsorbent for the removal of MO from aqueous solution. The experimental parameters, including surface chemistry, solution pH, particle size, adsorbent dosage, isotherm models, adsorption kinetics, and thermodynamics, were investigated to study the adsorption process. FTIR spectroscopy studies showed that the acidic groups, carboxyl and hydroxyl, were predominant contributors in MO uptake.

The experimental results show that the optimum conditions of adsorption were pH 2.0, absorbent dosage 5 g l^{-1} at 298 K for 120 min. The equilibrium data were correlated reasonably well by Langmuir adsorption isotherm. The maximum adsorption capacity of 16.66 mg g^{-1} was exhibited by cork. Moreover, the kinetic data suggest that the pseudo-second-order model well fitted the experimental results. Equilibrium adsorption capacity decreases with the increasing temperature. The adsorption thermodynamics indicate that the adsorption of MO onto cork is spontaneous and exothermic.

As a low-cost natural abundant adsorbent material, cork may be an alternative to more costly adsorbent materials.

References

[1] S. Vinitnantharat, W. Chartthe, A. Pinisakul, Toxicity of reactive red 141 and basic red 14 to algae and water fleas, Water Sci. Technol. 58 (2008) 1193–1198.
[2] M. Ma, F. Shen, X. Lu, W. Bao, H. Ma, Studies on the adsorption behavior of methyl orange from dye wastewater onto activated clay, Desalin. Water Treat. 51 (2013) 3700–3709.
[3] Y. Xu, R.E. Lebrun, Treatment of textile dye plant effluent by nanofiltration membrane, Sep. Sci. Technol. 34 (1999) 2501–2519.
[4] T. Bechtold, E. Burtscher, A. Turcanu, Cathodic decolorisation of textile wastewater containing reactive dyes using multi-cathode electrolyser, J. Chem. Technol. Biotechnol. 76 (2001) 303–311.
[5] S. Papic, N. Koprivanac, A.L. Bozic, A. Metes, Removal some reactive dyes from synthetic wastewater by combined Al(III) coagulation/carbon adsorption process, Dyes Pigm. 62 (2004) 291–298.
[6] N. Akhtar, J. Iqbal, M. Iqbal, Enhancement of Lead(II) biosorption by microalgal biomass immobilized onto Loofa (*Luffa cylindrica*) sponge, Eng. Life Sci. 4 (2004) 171–178.
[7] S. Kahraman, D. Asma, S. Erdemoglu, O. Yesilada, Biosorption of Copper(II) by live and dried biomass of the white rot fungi *Phanerochaete chrysosporium* and *Funalia trogii*, Eng. Life Sci. 5 (2005) 72–77.
[8] L.V. Gonzalez-Gutierrez, E.M. Escamilla-Silva, Reactive red azo dye degradation in a UASB bioreactor: Mechanism and kinetics, Eng. Life Sci. 9 (2009) 311–316.
[9] S. Karcher, A. Kornmüller, M. Jekel, Screening of commercial sorbents for the removal of reactive dyes, Dyes Pigm. 51 (2001) 111–125.
[10] P. Liu, L. Zhang, Adsorption of dyes from aqueous solutions or suspensions with clay nano-adsorbents, Sep. Purif. Technol. 58 (2007) 32–39.
[11] M. Arami, N. Yousefi-Limaee, N.M. Mahmoodi, N. Salman-Tabrizi, Equilibrium and kinetics studies for the adsorption of direct and acid dyes from aqueous solution by soy meal hull, J. Hazard. Mater. B135 (2006) 171–179.
[12] M. Turabik, Adsorption of basic dyes from single and binary component systems onto bentonite: Simultaneous analysis of basic red 46 and basic yellow 28 by first order derivative spectrophotometric analysis method, J. Hazard. Mater. 158 (2008) 52–64.

[13] C.C. Wang, L.C. Juang, T.C. Hsu, C.K. Lee, J.F. Lee, F.C. Huang, Adsorption of basic dyes onto montmorillonite, J. Colloid Interface Sci. 273 (2004) 80–86.
[14] K.K.H. Choy, J.F. Porter, G. Mckay, Intraparticle diffusion in single and multicomponent acid dye adsorption from wastewater onto carbon, Chem. Eng. J. 103 (2004) 133–145.
[15] I. Ali, V. Gupta, Advances in water treatment by adsorption technology, Nat. Protoc. 1 (2007) 2661–2667.
[16] A. Gil, F. Assis, S. Albeniz, S. Korili, Removal of dyes from wastewaters by adsorption on pillared clays, Chem. Eng. J. 168 (2011) 1032–1040.
[17] J.M. Chern, C.Y. Wu, Desorption of dye from activated carbon beds: Effects of temperature, pH, and alcohol, Water Res. 35 (2001) 4159–4165.
[18] T. Robinson, G. McMullan, R. Marchant, P. Nigam, Remediation of dyes in textile effluent: A critical review on current treatment technologies with a proposed alternative, Bioresour. Technol. 77 (2001) 247–255.
[19] M. Sadeghi-Kiakhani, M. Arami, K. Gharanjig, Dye Removal from colored-textile wastewater using chitosan-PPI dendrimer hybrid as a biopolymer: Optimization, kinetic, and isotherm studies, J. Appl. Polym. Sci. 127 (2013) 2607–2619.
[20] F.J. Guymont, I.H. Suffet, M.J. McGuire (Eds.), Activated Carbon Adsorption of Organics from Aqueous Phase, vol. 2, Ann Arbor Science, Ann Arbor, MI, 1984 (Chapter 23).
[21] A.K. Mittal, C. Venkobachar, Sorption and desorption of dyes by sulfonated coal, J. Environ. Eng. Div. 119 (1993) 366–368.
[22] D. Sun, X. Zhang, Y. Wu, X. Liu, Adsorption of anionic dyes from aqueous solution on fly ash, J. Hazard. Mater. 181 (2010) 335–342.
[23] F. Ferrero, Dye removal by low cost adsorbents: Hazelnut shells in comparison with wood sawdust, J. Hazard. Mater. 142 (2007) 144–152.
[24] M.S. El-Geundi, Color removal from textile effluents by adsorption technique, Water Res. 25 (1991) 271–273.
[25] I.D. Mall, V.C. Srivastava, N.K. Agarwal, Removal of orange-G and methyl violet dyes by adsorption onto bagasse fly ash and kinetic study and equilibrium isotherm analyses, Dyes Pigm. 69 (2006) 210–223.
[26] I.D. Mall, V.C. Srivastava, N.K. Agarwal, I.M. Mishra, Removal of congo red from aqueous solution by bagasse fly ash and activated carbon: Kinetic study and equilibrium isotherm analyses, Chemosphere 61 (2005) 492–501.
[27] V.S. Mane, I.D. Mall, V.C. Srivastava, Use of bagasse fly ash as an adsorbent for the removal of brilliant green dye from aqueous solution, Dyes Pigm. 73 (2006) 269–278.
[28] L.S. Balistrieri, J.W. Murray, The surface chemistry of goethite (α-FeOOH) in major ion seawater, Am. J. Sci. 281 (1981) 788–806.
[29] S.L. Goertzen, K.D. Thériault, A.M. Oickle, A.C. Tarasuk, H.A. Andreas, Standardization of the Boehm titration. Part I. CO_2 expulsion and endpoint determination, Carbon 48 (2010) 1252–1261.
[30] I. Langmuir, The adsorption of gases on plane surfaces of glass, mica and platinum, J. Am. Chem. Soc. 40 (1918) 1361–1368.
[31] H. Freundlich, Adsorption in solution, Phys. Chem. Soc. 40 (1906) 1361–1368.
[32] A. Özcan, E.M. Öncü, A.S. Özcan, Kinetics, isotherm and thermodynamic studies of adsorption of acid blue 193 from aqueous solutions onto natural sepiolite, Colloids Surf., A 277 (2006) 90–97.
[33] B.K. Nandi, A. Goswami, M.K. Purkait, Adsorption characteristics of brilliant green dye on kaolin, J. Hazard. Mater. 161 (2009) 387–395.
[34] G. Crini, P.-M. Badot, Application of chitosan, a natural aminopolysaccharide, for dye removal from aqueous solutions by adsorption processes using batch studies: A review of recent literature, Prog. Polym. Sci. 33 (2008) 399–447.
[35] B.K. Nandi, A. Goswami, M.K. Purkait, Removal of cationic dyes from aqueous solutions by kaolin: Kinetic and equilibrium studies, Appl. Clay Sci. 42 (2009) 583–590.
[36] F. Krika, N. Azzouz, M.C. Ncibi, Adsorptive removal of cadmium from aqueous solution by cork biomass: Equilibrium, dynamic and thermodynamic studies, Arab. J. Chem. (in press), doi: 10.1016/j.arabjc.2011.12.013.
[37] M. Arami, N.Y. Limaee, N.M. Mahmoodi, N.S. Tabrizi, Removal of dyes from colored textile wastewater by orange peel adsorbent: Equilibrium and kinetics studies, J. Colloid Interface Sci. 288 (2005) 371–376.
[38] C. Namasivayam, D. Kavitha, Removal of congo red from water by adsorption onto activated carbon prepared from coir pith, an agricultural solid waste, Dyes Pigm. 54 (2002) 47–58.
[39] N.M. Mahmoodi, B. Hayati, M. Arami, C. Lan, Adsorption of textile dyes on Pine Cone from colored wastewater: Kinetic, equilibrium and thermodynamic studies, Desalination 268 (2011) 117–125.
[40] M.R. Malekbala, S. Hosseini, S.K. Yazdi, S.M. Soltani, M.R. Malekbala, The study of the potential capability of sugar beet pulp on the removal efficiency of two cationic dyes, Chem. Eng. Res. Des. 90 (2012) 704–712.
[41] R. Slimani, I. Ouahabi, F. Abidi, M. El Haddad, A. Regti, M.R. Laamari, S. El Antri, S. Lazar, Calcined eggshells as a new biosorbent to remove basic dye from aqueous solution: Thermodynamics, kinetics, isotherms and error analysis, J. Tai. Inst. Chem. Eng. 45 (2014) 1578–1587.
[42] M.A.M. Salleh, D.K. Mahmoud, W.A.W. Abdul Karim, A. Idris, Cationic and anionic dye adsorption by agricultural solid wastes: A comprehensive review, Desalination 280 (2011) 1–13.
[43] R. Liu, K. Fu, B. Zhang, D. Mei, H. Zhang, J. Liu, Removal of methyl orange by modified halloysite nanotubes, J. Dispersion Sci. Technol. 33 (2012) 711–718.
[44] Y. Iida, T. Kozuka, T. Tuziuti, K. Yasui, Sonochemically enhanced adsorption and degradation of methyl orange with activated aluminas, Ultrasonics 42 (2004) 635–639.
[45] L. Ai, J. Jiang, Fast removal of organic dyes from aqueous solutions by AC/ferrospinel composite, Desalination 262 (2010) 134–140.
[46] F. Atmani, A. Bensmaili, A. Amrane, Methyl orange removal from aqueous solutions by natural and treated skin almonds, Desalin. Water Treat. 22 (2010) 174–181.

[47] Q. Ma, F. Shen, X. Lu, W. Bao, H. Ma, Studied on the adsorption behavior of methyl orange from dye wastewater onto activate clay, Desalin. Water Treat. 51 (2013) 3700–3709.
[48] T.K. Saha, N.C. Bhoumik, S. Karmaker, M.G. Ahmed, H. Ichikawa, Y. Fukumori, Adsorption of methyl orange onto chitosan from aqueous solution, J. Water Res. Protect. 2 (2002) 898–906.
[49] A. Mittal, A. Malviya, D. Kaur, J. Mittal, L. Kurup, Studies on the adsorption kinetics and isotherms for the removal and recovery of methyl orange from wastewaters using waste materials, J. Hazard. Mater. 148 (2007) 229–240.
[50] Y. Su, Y. Jiao, C. Dou, R. Han, Biosorption of methyl orange from aqueous solutions using cationic surfactant-modified wheat straw in batch mode, Desalin. Water Treat. 52 (2014) 6145–6155.
[51] Y.J. Yao, B. He, F.F. Xu, X.F. Chen, Equilibrium and kinetic studies of methyl orange adsorption on multi-walled carbon nanotubes, Chem. Eng. J. 170 (2011) 82–89.
[52] I.D. Mall, V.C. Srivastava, G.V. Kumar, G.V.A.I.M. Mishra, Characterization and utilization of mesoporous fertilizer plant waste carbon for adsorptive removal of dyes from aqueous solution, Colloids Surf., A 278 (2006) 175–187.
[53] S. Lagergren, About the theory of so-called adsorption of soluble substances, K. Svenska Vetenskapsakad. Handl., 24 (1898) 1–39.
[54] Y.S. Ho, G. McKay, Pseudo-second-order model for sorption processes, Process Biochem. 34 (1999) 451–465.
[55] S.H. Chien, W.R. Clayton, Application of Elovich equation to the kinetics of phosphate release and sorption on soils, Soil Sci. Soc. Am. J. 44 (1980) 265–268.
[56] M.J. Jaycock, G.D. Parfitt, Chemistry of Interfaces, Ellis Horwood Ltd., Onichester, 1981.